Broadband Lossless Matching Layer for Lens Arrays at THz Frequencies

Bueno , J.; Bosma, S.; Bußkamp-Alda, T.; Alonso Del Pino, M.; Llombart, N.

DOI
10.1109/IRMMW-THz50927.2022.9895659

Publication date
2022

Document Version
Final published version

Published in
Proceedings of the 2022 47th International Conference on Infrared, Millimeter and Terahertz Waves (IRMMW-THz)

Citation (APA)
Bueno , J., Bosma, S., Bußkamp-Alda, T., Alonso Del Pino, M., & Llombart, N. (2022). Broadband Lossless Matching Layer for Lens Arrays at THz Frequencies. In *Proceedings of the 2022 47th International Conference on Infrared, Millimeter and Terahertz Waves (IRMMW-THz)* (pp. 1-2). IEEE. https://doi.org/10.1109/IRMMW-THz50927.2022.9895659

2022 47th International Conference on Infrared, Millimeter and Terahertz Waves (IRMMW-THz) | 978-1-7281-9427-1/22/$31.00 ©2022 IEEE | DOI: 10.1109/IRMMW-THz50927.2022.9895659

Broadband Lossless Matching Layer for Lens Arrays at THz Frequencies

J. Bueno[1,*], S. Bosma[2], T. Bußkamp-Alda[3], M. Alonso-delPino[2], and N. Llombart[2]
[1] Electronic Circuits and Architectures Group, Delft University of Technology, Delft, The Netherlands
[2] Tera-Hertz Sensing Group, Delft University of Technology, Delft, The Netherlands
[3] Veld Laser Innovations B.V., 's-Heerenberg, The Netherlands
j.buenolopez@tudelft.nl

***Abstract*— We present the design, fabrication and characterization of a broadband lossless matching layer for shallow lens arrays. The matching layer we propose is based on silicon pyramids fabricated on top of the lens array by means of laser ablation. This matching layer has the advantage that it covers over an octave of bandwidth. We have compared the performance of this matching layer with the commonly used parylene-C matching layer at the center of the targetted band, 500 GHz. The matching layer based on the silicon pyramids has 1.6 dB higher transmission.**

I. INTRODUCTION

SILICON is widely used for submillimeter-wave integrated lens antennas [1]-[3]. However, the high permittivity of silicon ($\varepsilon_r^{Si} = 11.9$) results in high reflection at the lens-air interface. These reflections negatively impact the sidelobes [3], [4] decrease the gain [4] and have a strong impact on the input impedance [5]. Numerous anti-reflection coatings (also known as matching layers, ML) have been developed to limit these reflections [6]-[9]. However, the coating materials themselves may incur additional dielectric losses, which may not be negligible at submillimeter wavelengths. Furthermore, the adhesion of the matching layers to the silicon lens can be difficult, especially for cryogenically cooled lenses. Periodic sub-wavelength structures in the same material (silicon) as the lens have been used as matching layers in the past [10]-[13]. However, there is not direct comparison between the performance of a quarter-wavelength AR coating and a continuous impedance-transforming matching layer in an integrated silicon lens antenna.

II. LENS MATCHING LAYER ANALYSIS

We compare the simulated performance of two matching layers on the silicon lens antenna described in [14] in the operational bandwidth of this antenna of 450-650 GHz: a quarter-wavelength (94 μm) layer of parylene-C and a periodic arrangement of sub-wavelength flat-topped square pyramids in silicon. The pyramids are fabricated using laser ablation at Veld Laser Innovations B.V. (www.veldlaser.nl). Due to the small dimensions of the pyramids, this micro-fabrication technique has two constrains for the design: i) it is not possible to carve straight walls in the silicon. The minimum angle that can be obtained for these specific pyramid dimensions is 13 degrees. This is not a problem since we want a broadband matching layer and the tapered walls increase the bandwidth; ii) it is very difficult to end the pyramids a sharp point at the top reliably for the whole lens array. We therefore decided to truncate the top of the pyramids and form a frusta instead. These dimensions are given in [15] for a higher frequency design (2 THz) and have been scaled to 500 GHz to meet our frequency band. The design values can be found in Table I. The simulated transmission of both the parylene-C and frustra matching layers are given in Fig. 1. They are better than -0.3 dB for both structures in the center of the band but the parylene-C ML transmission decays for lower and higher frequencies whereas the pyramid ML stays fairly constant for the full bandwidth.

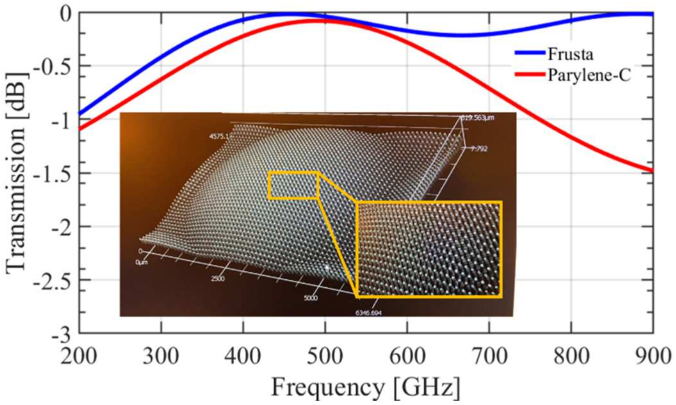

Fig. 1. Simulated transmission of both the parylene-C and the periodic frusta matching layer. The inset shows a 3D image of the central lens and zoomed view of the frusta.

III. CHARACTERIZATION OF THE FABRICATED AR COATING

The lens array is fabricated in two steps. First, the full lens array is manufactured thicker than the lens nominal design. Secondly, this extra thickness will be carved later and become the pyramids. These two steps are fabrication is performed in the same laser setup but with two different settings. The lens array is made using a 3D file, where the laser follows its profile. Afterwards, the setup is changed to a 2D mode and the grid where the excess material will be removed is defined. The frusta are carved by passing the laser several times to obtain the correct depth. It is not possible to carve the frusta conformally using this technique but this is not a problem since the lenses are very shallow. The frusta of the matching layer are measured using a confocal microscope (Fig. 1). This type of microscope takes 2D images of the surface at different depths, enabling the reconstruction of the 3D image. The 3D images can be sliced and used to measure the profile of the frusta, and therefore obtain their period, their dimension of the top flat part and their height.

978-1-7281-9427-1/22/$31.00 ©2022 IEEE

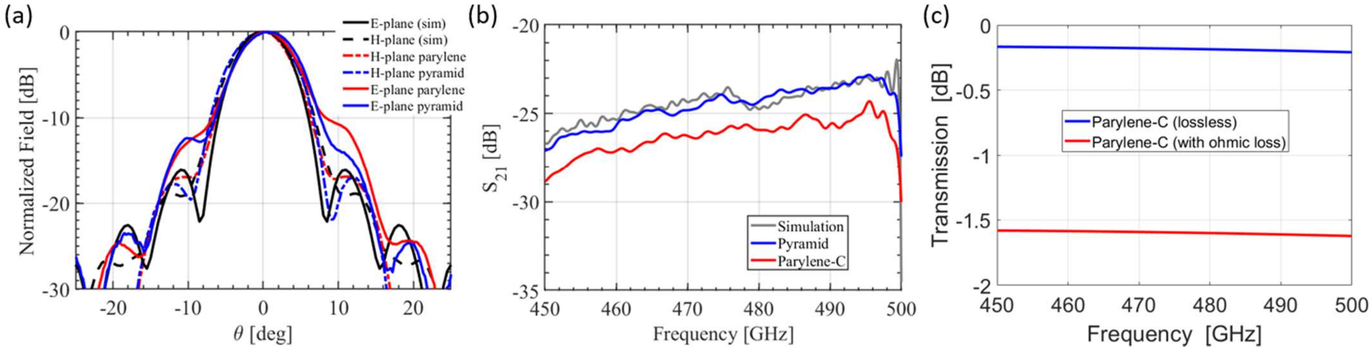

Fig. 2. a) Simulated and measured beam patterns. b) Simulated and measured S_{12}. c) Simulated loss of the parylene-C matching layer with added ohmic loss.

IV. MEASUREMENTS AND RESULTS

The lens arrays are integrated and measured one-by-one in a lens antenna fed by a high-efficiency leaky-wave feed described in [14]. We measure the antenna between 450 and 500 GHz using a VNA and two WR-2.2 frequency extenders. The antenna under test is in a fixed position and the receiving antenna placed in a 3-axis CNC stage. The antenna patterns in the far field at 10 cm distance are measured using an open-ended waveguide flange with eccosorb material surrounding the waveguide aperture on the flange, whereas the antenna gain is measured using a horn with a gain of around 20 dBi. The measured radiation pattern is compared to the simulated pattern at 480 GHz (Fig. 2a). The measurements are in good agreement with the simulated patterns. The patterns from the parylene-C and pyramid matching layer are nearly identical, indicating similar directivity. We use Friis' equation to simulate the coupling between the antenna and horn (S_{12}) at broadside. The measured coupling is in very good agreement for the frusta matching layer but ~1.6dB lower for the parylene-C matching layer (Fig. 2b). This difference can be explained by the ohmic loss present in the parylene-C (Fig. 2c), where an absorption coefficient of 35cm^{-1} is used [16].

V. DISCUSSION AND CONCLUSIONS

We compare the performance at submillimeter wavelengths of two different matching layers on the same silicon leaky-wave lens antenna. The fabricated antennas are the same with the exception of the matching layer. We describe the commercial laser ablation process used to create the frusta matching layer. The measured gain of the antenna with frusta matching layer is ~1.6 dB higher than with the parylene-C matching layer. The difference is explained by the dielectric loss of the parylene-C, which is in line with the absorption coefficient in the literature. Furthermore, the frusta matching layer operates over more than an octave bandwidth.

ACKNOWLEDGMENTS

This work has been supported by the ERC starting grant, Lens Antenna Arrays for Coherent THz Cameras (LAA-THz-CC, 639749).

REFERENCES

[1] D. F. Filipovic, S. S. Gearhart, and G. M. Rebeiz, "Double-slot antennas on extended hemispherical and elliptical silicon dielectric lenses," *IEEE Transactions on Microwave Theory and Techniques*, vol. 41, no. 10, pp. 1738–1749, (1993)

[2] N. Llombart, G. Chattopadhyay, A. Skalare, and I. Mehdi, "Novel Terahertz Antenna Based on a Silicon Lens Fed by a Leaky Wave Enhanced Waveguide," *IEEE Transactions on Antennas and Propagation*, vol. 59, no. 6, pp. 2160–2168 (2011)

[3] M. Alonso-delPino, C. Jung-Kubiak, T. Reck, N. Llombart, and G. Chattopadhyay, "Beam Scanning of Silicon Lens Antennas Using Integrated Piezomotors at Submillimeter Wavelengths," *IEEE Transactions on Terahertz Science and Technology*, vol. 9, no. 1, pp. 47–54 (2019)

[4] N. T. Nguyen, R. Sauleau, and C. J. Martinez Perez, "Very Broadband Extended Hemispherical Lenses: Role of Matching Layers for Bandwidth Enlargement," *IEEE Transactions on Antennas and Propagation*, vol. 57, no. 7, pp. 1907–1913 (2009)

[5] A. Neto, L. Borselli, S. Maci, and P. J. I. D. Maagt, "Input impedance of integrated elliptical lens antennas," *IEE Proceedings - Microwaves, Antennas and Propagation*, vol. 146, no. 3, pp. 181–186 (1999)

[6] A. J. Gatesman, J. Waldman, M. Ji, C. Musante, and S. Yagvesson, "An anti-reflection coating for silicon optics at terahertz frequencies," *IEEE Microwave and Guided Wave Letters*, vol. 10, no. 7, pp. 264–266 (2000)

[7] S. Sahin, N. K. Nahar, and K. Sertel, "Thin-Film SUEX as an Antireflection Coating for mmW and THz Applications," *IEEE Transactions on Terahertz Science and Technology*, vol. 9, no. 4, pp. 417–421 (2019)

[8] J. Lau et al., "Millimeter-wave antireflection coating for cryogenic silicon lenses," *Appl. Opt., AO*, vol. 45, no. 16, pp. 3746–3751 (2006)

[9] A. Neto, S. Monni, and F. Nennie, "UWB, Non Dispersive Radiation From the Planarly Fed Leaky Lens Antenna—Part II: Demonstrators and Measurements," *IEEE Transactions on Antennas and Propagation*, vol. 58, no. 7, pp. 2248–2258 (2010)

[10] R. Datta et al., "Large-aperture wide-bandwidth antireflection-coated silicon lenses for millimeter wavelengths," *Appl. Opt., AO*, vol. 52, no. 36, pp. 8747–8758 (2013)

[11] T. Hasebe et al., "Development of Multi-Layer Anti-Reflection Structures for Millimeter-Wave Silicon Optics Using Deep Reactive Ion Etching Process," *J Low Temp Phys*, vol. 199, no. 1, pp. 339–347 (2020)

[12] K. Young et al., "Broadband millimeter-wave anti-reflection coatings on silicon using pyramidal sub-wavelength structures," *Journal of Applied Physics*, vol. 121, no. 21, p. 213103 (2017)

[13] T. Nitta et al., "Design, Fabrication and Measurement of Pyramid-Type Antireflective Structures on Columnar Crystal Silicon Lens for Millimeter-Wave Astronomy," *J Low Temp Phys*, vol. 193, no. 5, pp. 976–983 (2018)

[14] M. Alonso-delPino, S. Bosma, C. Jung-Kubiak, G. Chattopadhyay, and N. Llombart, "Wideband Multimode Leaky-Wave Feed for Scanning Lens-Phased Array at Submillimeter Wavelengths*," IEEE Transactions on Terahertz Science and Technology*, vol. 11, no. 2, pp. 205–217 (2021)

[15] O. Yurduseven, "Wideband Integrated Lens Antennas for Terahertz Deep Space Investigation," *PhD* Thesis, Delft University of Technology (2016)

[16] H.-W Hübers, J Schubert, A Krabbe, M Birk, G Wagner, A Semenov, G Gol'tsman, B Voronov, E Gershenzon, "Parylene anti-reflection coating of a quasi-optical hot-electron-bolometric mixer at terahertz frequencies", *Infrared Physics & Technology*, vol. 42, no. 1, pp. 41-47 (2001)